Geochronological and geochemical features of the Cathaysia block (South China): new evidence for the Neoproterozoic breakup of Rodinia

Liangshu S. Shu, Michel Faure, Jinhai Yu, Bor-Ming Jahn

Geochronological and geochemical features of the Cathaysia block (South China): New evidence for the Neoproterozoic breakup of Rodinia

Liang-Shu Shu[a] , Michel Faure[b], Jin-Hai Yu[a], Bor-Ming Jahn[c]

[a] State Key Laboratory for Mineral Deposits Research, Nanjing University, Nanjing 210093, China

[b] Institut des Sciences de la Terre d'Orléans, UMR 6113 – CNRS/Université d'Orléans, 1A, rue de la Férollerie, 45071 Orléans Cedex 2, France

[c] Department of Geosciences, National Taiwan University, P.O. Box 13-318, Taipei 106, Taiwan

Abstract

The Cathaysia block is an important element for the reconstruction of the Proterozoic tectonic evolution of South China within the Rodinia supercontinent. The Pre-Devonian Cathaysia comprises two litho-tectonic units: a low-grade metamorphic unit and a basement unit; the former was a late Neoproterozoic–Ordovician sandy and muddy sedimentary sequence, the latter consists essentially of metamorphosed Neoproterozoic marine facies sedimentary and basaltic rocks, and a subordinate amount of Paleoproterozoic granites and amphibolites. This block has undergone several tectono-magmatic events. The first event occurred in the late Paleoproterozoic, at ca. 1.9–1.8 Ga, and the tectonic–magmatic event dated at 0.45–0.40 Ga was resulted from the early Paleozoic orogeny that made the Pre-Devonian rocks to undergo a regional lower greenschist to amphibolite facies metamorphism. The Neoproterozoic geodynamic event is poorly understood. In this paper, new U–Pb zircon age, whole-rock chemical and zircon Hf isotopic data for mafic and felsic igneous rocks are used to constrain the tectonic evolution of Cathaysia. Zircon SHRIMP U–Pb analyses on four mafic samples yielded rather similar Neoprotorozoic ages of 836 ± 7 Ma (gabbro), 841 ± 12 Ma (gabbro), 847 ± 8 Ma (gabbro) and 857 ± 7 Ma (basalt). Combined with the published isotopic age data, most of the mafic samples dated at 800–860 Ma show geochemical characteristics of continental rift basalt. By contrast, rhyolitic samples with an age of 970 Ma have a volcanic arc affinity. All mafic samples have LREE-enriched REE patterns, and non-ophiolitic trace element characteristics. However, the zircon Hf isotopic data of mafic samples show positive epsilon $\varepsilon_{Hf}(t)$ values (+4.1 to +10.5), suggesting that they were originated from a long-term depleted mantle source. All the available ages indicate that the Cathaysia block has registered two stages of Neoproterozoic magmatism. The younger stage corresponds to a continental rifting phase with emplacement of mafic rocks during the period of 860–800 Ma, whereas the older stage represents an eruption of volcanic arc rocks at about 970 Ma. These two magmatic stages correspond to two distinct tectonic settings within the framework of the geodynamic evolution of Cathaysia. Such a similar Neoproterozoic stratigraphy and magmatism between the Cathaysia, Yangtze and Australian blocks provide a significant line of evidence for placing the Cathaysia block within the Rodinia supercontinent.

Keywords : SHRIMP U–Pb zircon dating; Geochemistry and Hf isotope; Mafic igneous rocks; Rhyolite; Neoproterozoic rifting; Cathaysia block; South China

1. Introduction

The reconstruction of supercontinents is an important geodynamic issue with regard to the Precambrian global tectonic framework and geological evolution. Studies of the assembly and break-up of Rodinia in the Meso- to Neoproterozoic period have been significantly advanced in recent years (Hoffman, 1991 and Li et al., 2008b and enclosed references). However, the Precambrian tectonic evolution of the Cathaysia block of China is still poorly understood.

The South China Block (SCB) is composed of the Cathaysia and Yangtze sub-blocks (called commonly the Cathaysia block and the Yangtze block in literatures), which have been considered as two separate members of the Neoproterozoic Rodinia supercontinent (Li et al., 1995). Previous works suggest that similar Neoproterozoic stratigraphic successions and magmatic rocks exist between the Yangtze and the Australian continents (Li et al., 1996 and Wang and Li, 2003). This seems to provide a strong argument for the involvement of the Yangtze block in the Rodinia supercontinent, from assembly to breakup during the Neoproterozoic. On the other hand, due to the lack of geochronological and geochemical data, the link between the Cathaysia block and Rodinia has not been established like between the Yangtze block and Rodinia.

Cathaysia is separated from the Yangtze block by a Neoproterozoic ophiolitic suture (Xu and Qiao, 1989, Shu et al., 1994 and Shu and Charvet, 1996) along the Shaoxing–Jiangshan–Pingxiang fault. The Shaoxing–Jiangshan–Pingxiang fault has been considered as a collisional zone between the Yangtze and Cathaysia blocks during the early Neoproterozoic, around 900 Ma (Shu et al., 1994, Li et al., 2002b, Li et al., 2003a, Li et al., 2008a, Li et al., 2009, Ye et al., 2007 and Yao et al., 2011). The NE-trending Zhenghe–Dapu fault zone occurs within the Cathaysia block, and cuts Neoproterozoic rocks of Cathaysia (Fig. 1). Neoproterozoic muddy to sandy sediments and volcanic rocks are distributed both sides of the Zhenghe–Dapu fault. The fossil-bearing Carbo-Permian and Cambro-Ordovician sequences have also been identified on both sides of the Zhenghe–Dapu fault (Lu et al., 1994, Yu, 1994 and Shu et al., 2009). Some mafic–ultramafic and bimodal igneous rocks with a late Neoproterozoic age were swarmed within the fault zone.

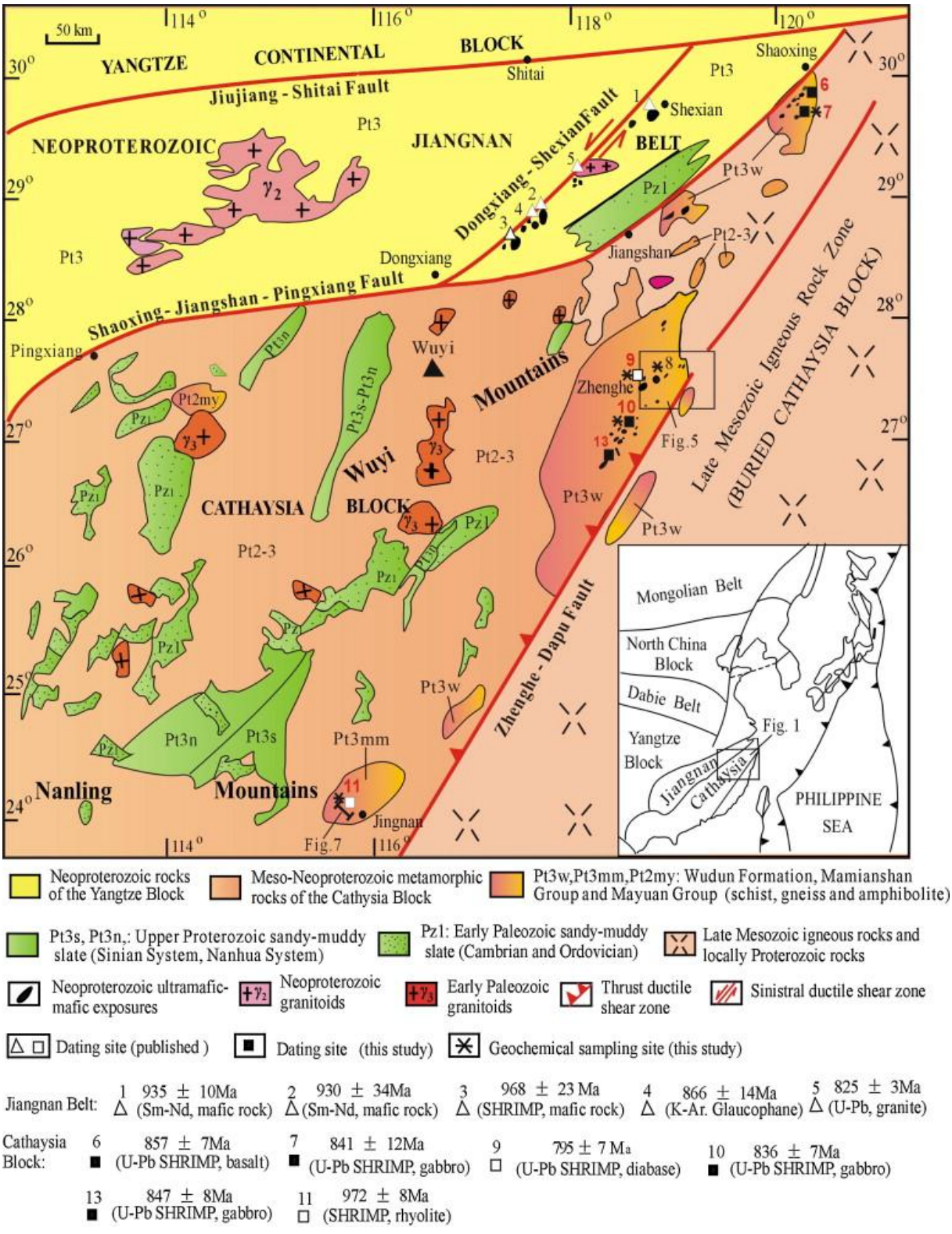

Fig. 1. Simplified geological map of the Cathaysia block, South China.

Neoproterozoic tectono-magmatic record (mafic, ultramafic and acidic magmatic rocks) and locally Meso-Paleoproterozoic basement are well preserved in the Wuyi and Nanling Mts. (Fig. 1; Shu, 2006, Wan et al., 2007, Yu et al., 2009 and Yao et al., 2011). The Neoproterozoic sedimentary sequence contains some olistostrome features, such as various blocks with different components, sizes, shapes and ages that were interpreted as an intra-block rift formed in response to the breakup of the Rodinia supercontinent (Wang and Li, 2003). However, the detailed timing and geological setting of this olistostrome formation are unclear.

In the past two decades, numerous studies suggested that a Proterozoic basement exists in the Cathaysia block. U–Pb protolith ages, ranging from 1000 Ma to 800 Ma, obtained from igneous rocks were regarded to be related to the assembly and breakup of Rodinia (Li et al., 2005, Wan et al., 2007, Xu et al., 2005, Xu et al., 2007, Shu, 2006, Shu et al., 2008a and Li et al., 2010b). Moreover, some geochronological data from zircon grains from amphibolites and gneisses imply that the 1.9–1.8 Ga event was an important period for the formation of the oldest metamorphic basement of Cathaysia (Wan et al., 2007 and Yu et al., 2008). In spite of the significant advance in geochronology, controversies still exist on the onset of the rifting event between Cathaysia and other parts of Rodinia (Li et al., 2009, Wang et al., 2003, Wang et al., 2008a, Wang et al., 2008b and Xiang and Shu, 2010).

Mafic–ultramafic rocks are exposed as lenses (meter to hundred-meter size) in the upper part of the basement of the Cathaysia block. These rocks have attracted much attention and various models have been proposed: (1) an ophiolitic mélange formed by the subduction of an early Paleozoic South China Ocean (Guo et al., 1989 and Wang and Mo, 1995); (2) a late Paleozoic to early Mesozoic ophiolitic suture (Xiao and He, 2005); and (3) a disrupted Precambrian intra-continental magmatic dyke swarm (Shu et al., 2008a). However, the most serious problem for all the models is the insufficient age and geochemical constraints. Consequently, the origin and emplacement time of these mafic–ultramafic rocks have not been resolved.

In this paper, we address the question of the origin and timing of the emplacement of the mafic–ultramafic rocks and their tectonic implications. Petrological, geochronological and geochemical studies were conducted on some mafic and felsic rocks from the Proterozoic basement of Cathaysia. The new results will allow us to conclude that (1) these ultramafic–mafic rocks do not represent the relics of an ophiolitic suite, (2) they were formed in an intra-continental rift setting during middle Neoproterozoic, in response to the breakup of Rodinia, and (3) the Cathaysia block was an important tectonic unit of Rodinia.

2. Geological background of the Cathaysian block

2.1. Tectonic outline

The SCB has undergone several tectono-magmatic events. The first event occurred in the late Paleoproterozoic, at ca. 1.9–1.8 Ga. This event has been argued as the most important one in the formation of the crystalline basement of Cathaysia (Wan et al., 2007 and Yu et al., 2009). However, no structural evidence associated with this magmatic event is available. The second event took place during the early Neoproterozoic as a result of the collision between the Yangtze and Cathaysia blocks (Guo et al., 1989, Li et al., 1994, Shu and Charvet, 1996, Charvet et al., 1996, Chen et al., 1997 and Li et al., 1999). The time of collision is constrained by available age data for rocks from the suture zone, including zircon U–Pb ages of 968–930 Ma for mafic rocks from the ophiolite (Xu and Qiao, 1989, Zhou and Zhu, 1993, Chen et

al., 1991 and Li et al., 1994), a glaucophane K–Ar age of 886 ± 14 Ma for blueschist (Shu et al., 1994), and several zircon U–Pb ages of 830–800 Ma for S-type granitoids (Li et al., 2003a and Zheng et al., 2008). The age of 1020–930 Ma corresponds to the subduction time of the Proto-South China Ocean (Zhou and Zhu, 1993, Zhou et al., 2002, Zhou et al., 2004 and Zhou et al., 2009), the 866 ± 14 Ma age might represents the time of collision (Charvet et al., 1996), and the 850–800 Ma age was considered as the time of post-collisional magmatism or a consequence of the breakup of Rodinia (Li et al., 2008b, Li et al., 2009 and Li et al., 2010a).

As documented in the following sections, a Neoproterozoic tectono-magmatic event occurred also within the Cathaysia block along the Zhenghe–Dapu fault zone.

The Silurian sequence is absent in the Cathaysia block due to an uplift since the late Ordovician. The uplift was a response to the early Paleozoic tectono-magmatic event. This event that welded again the Cathaysia and Yangtze blocks, is marked by an important deformation with regional-scale folding and faulting and granitic magmatism (Shu et al., 2008c, Faure et al., 2009 and Charvet et al., 2010). The termination of the orogeny is indicated by unconformable deposition of middle to late Devonian molasse of 1–2 km thickness. Recent studies have revealed a top-to-the-south ductile decollement and widespread crustal melting at about 450–400 Ma (Wang et al., 2003, Wang et al., 2007 and Faure et al., 2009). Locally, a top-to-the-north ductile shearing was recently observed in the areas near or to the north of the Shaoxing–Jiangshan–Pingxiang fault (Shu et al., 2008c and Charvet et al., 2010). This early Paleozoic orogenic event reworked the geographic framework of Cathaysia (Rong et al., 2010), and is interpreted as an intra-continental orogeny within the SCB (Shu et al., 2008c, Faure et al., 2009 and Li et al., 2010b).

Two major litho-tectonic units can be recognized in the Cathaysia block: a low-grade metamorphic unit and a basement unit. The low-grade metamorphic unit is represented by a late Neoproterozoic to Ordovician sandstone–mudstone slaty sequence. The basement unit is composed of early Neoproterozoic sandstone, mudstone and volcanic rocks in the Nanling–Yunkai area and Paleoproterozoic granites, metasedimentary and volcanic rocks in eastern Cathaysia (Wuyishan segment) (JBGMR, 1984, FBGMR, 1985, Li, 1997 and Yu et al., 2009) that were later metamorphosed into micaschist, amphibolite and gneiss (Yu et al., 2008 and Li et al., 2010b).

2.2. Petrotectonic assemblages of the basement unit

The basement unit is also called the pre-Nanhua System in the Chinese literature. It is composed mainly of Neoproterozoic marine facies sedimentary and basaltic rocks, and a subordinate amount of Paleoproterozoic granites and metamorphic rocks (including amphibolites in the Tianjingping formation and migmatites and gneisses in the Badu Group) (Li, 1997 and Yu et al., 2009). Late granitoids intruded the Neoproterozoic rocks (JBGMR, 1984 and FBGMR, 1985). The protolith of the meta-volcanic rocks was dated at 1000–800 Ma (Wan et al., 2007, Shu et al., 2008a and Li et al., 2010a), whereas the Paleoproterozoic granites and amphibolites were dated at 1890–1766 Ma by zircon U–Pb method (Li, 1997, Gan et al., 1995, Yu et al., 2009, Li et al., 2000 and Li et al., 2010b). In Fujian Province, the pre-Nanhua System is composed of the Wudun Formation (Pt_3w), Mamianshan Group (Pt_3mm) and Mayuan Group (Pt_2my) (FBGMR, 1985 and Gan et al., 1995).

The Wudun Formation, which is equivalent to the Chencai Group of Zhejiang Province and the Zhoutan Group (or Shenshan Group) of Jiangxi Province, is mainly composed of meta-sedimentary and meta-basatic and ultramafic rocks (Wan et al., 2007). Some ultramafic and mafic blocks were dated at 850–800 Ma by SHRIMP U–Pb method on zircon (Li et al., 2005 and this study; see Section 3).

The Mamianshan Group of the pre-Nanhua System, is equivalent to the Longquan Group of Zhejiang Province or the Tieshajie Group of Jiangxi Province. The Mamianshan Group is composed of meta-sedimentary and meta-volcanic rocks (JBGMR, 1984, FBGMR, 1985 and Li et al., 2005), with a small amount of quartzite, amphibolite and marble. These rocks are exposed in two areas: Wuyi and Nanling (Fig. 1). Zircons from the granitic gneiss (paragneiss) of the Nanling area were subject to age determination (Yu et al., 2007). The SHRIMP zircon U–Pb age of 972 ± 8 Ma from a 60 m thick rhyolite section in Nanling is consistent with this Group (Shu et al., 2008b).

The Mayuan Group is exposed only in the Wuyi Mts. It was thought to be equivalent to the Badu Group of Zhejiang Province, and is composed of meta-sedimentary and meta-volcanic rocks, such as, biotite-schist, paragneiss, quartzite and migmatite (Wan et al., 2007). The protoliths of this Group were previously assigned to the Paleoproterozoic (FBGMR, 1985 and Gan et al., 1995) and are considered as the oldest rocks found in the Cathaysia Block (Yu et al., 2009). Paleoproterozoic granites and metamorphic rocks of the Badu Group are widely developed in the northern Wuyishan segment of the Cathaysia block. In the Longquan area of southern Zhejiang, five granitic plutons that intruded the Badu Group yielded significant dating values by LA-ICPMS zircon U–Pb method, namely, 1888 ± 7 Ma (Xiaji pluton), 1875 ± 9 Ma (Lizhuang granite), 1867 ± 8 Ma (Wangyu gneissic granite), 1855 ± 8 Ma (Danzhu granite) and 1856 ± 10 Ma (Tianhou pluton), respectively (Yu et al., 2009). Two groups of zircon U–Pb upper intercept ages for metamorphic rocks in the Longyou County also were reported, for example, 1924 ± 31 Ma (Gan et al., 1995) for the Xinquan banded migmatite and 1868 ± 8 Ma (Yu et al., 2009) for the Xikou gneiss near Xinquan. These isotopic dating data indicate that a magmatism and metamorphism took place in the period of 1900–1850 Ma. Combined with geochemical signatures of these granites and metamorphic rocks, the Paleoproterozoic tectonothermal event in the Cathaysia block can link to a Paleoproterozoic orogeny that coincides with the assembly of the supercontinent Columbia, suggesting that the Cathaysia block likely was a member of this supercontinent.

Like the Mayuan Group, the Tianjingping Formation crops out in the Wuyi Mts., and consists of similar lithological units (garnet–mica-schist, biotite–amphibole gneiss, amphibolite and granitic gneiss). The amphibolite was dated at 1766 ± 19 Ma by the SHRIMP U–Pb zircon method (Li, 1997); and this date was interpreted as the protolith age. The available age data suggest that a magmatic and metamorphic event took place around 1.9–1.8 Ga (Xu et al., 2007, Wan et al., 2007, Yu et al., 2009, Li et al., 2000 and Li et al., 2010b).

Furthermore, metatexites, diatexites and anatectic granitoids are well developed in the Cathaysia block. Although sometimes interpreted as pieces of the Precambrian basement, some migmatites from the basement unit yield “young” SHRIMP zircon U–Pb and monazite U–Th–Pb ages of ca 450–400 Ma (Wan et al., 2007, Faure et al., 2009 and Li et al., 2010b). These migmatites are considered as having formed during the early Paleozoic orogeny. Nevertheless, the distinction between Precambrian and Paleozoic migmatites is very difficult when radiometric dates are not available.

2.3. The low-grade metamorphic unit

The slightly metamorphic sequence consists of four Systems, from top to bottom: Ordovician System, Cambrian System, the late Neoproterozoic Sinian System, and the late Neoproterozoic Nanhua System. As a whole, the protoliths of the low-grade metamorphic unit were deposited in a long period from 800 to 444 Ma (Gradstein et al., 2004 and Zhang and Yan, 2005) and were metamorphosed in the period of about 450–400 Ma (Yu et al., 2005, Wan et al., 2007, Faure et al., 2009 and Li et al., 2010b). This unit consists mainly of sandstone and mudstone, with a subordinate amount of Neoproterozoic meta-volcanic rocks in the Nanhua System (Chen et al., 2010). There is no remarkable depositional discontinuity from the Neoproterozoic Nanhua System to the Ordovician System. The absence of lava flows is also a noticeable feature of the whole sequence of this unit (Shu, 2006, Shu et al., 2008a and Shu et al., 2008b).

The 5000 m thick Cambrian and Ordovician sedimentary sequences are characterized by neritic to bathyal facies sandy–muddy sedimentary rocks. The Sinian System, with a thickness of 300–500 m, is composed of phosphorus-bearing sandstone and mudstone. The lower part of this System contains matrix-supported conglomerates with poly-compositional pebbles. These pebbles show irregular shape and variable sizes; and they were considered as glaciers deposits (JBGMR, 1984). The Nanhua System consists of 1–2 km thick sandstone, pelite and conglomerate, and locally presents chaotic sedimentary features representative of an olistostrome. This succession is interpreted as having deposited in a rift environment (Wang and Li, 2003).

The late Neoproterozoic to Ordovician series underwent a regional lower greenschist facies metamorphism that changed the sandy–muddy rocks into chlorite–sericite slates during the Late Ordovician–Early Devonian orogeny dated at 450–400 Ma (Yu et al., 2008, Faure et al., 2009, Li et al., 2010b and Xiang and Shu, 2010). The late Ordovician graptolite sequence indicates a significant change from the deep-water graptolitic black shale to the rapidly accumulated, shallow-water clastic deposits, implying an initial timing of the early Paleozoic Orogeny (Chen et al., 2010).

The late Neoproterozoic to Ordovician sedimentary series was intruded by Silurian granitic plutons. Subsequently, the middle Devonian terrigenous sediments (mainly conglomerate and coarse-grained sandstone; non-metamorphosed) were deposited unconformably on the early Paleozoic rocks (Rong et al., 2003, Rong et al., 2010, Shu et al., 2006, Shu et al., 2008a, Shu et al., 2008b and Chen et al., 2010). This event marks the end of the early Paleozoic orogeny.

2.4. Mafic–ultramafic blocks

In the pre-Nanhua System of the Cathaysia block, mafic–ultramafic rocks are incorporated into a disrupted sequence of sedimentary and volcanic rocks with fragmented and discontinuous beds. Consequently, the entire lithological assemblage resembles an olistostrome. Several tens of mafic–ultramafic blocks with size ranging from tens of meters up to several hundred meters, occur in the Wudun Formation. They are scattered along or near the Zhenghe–Dapu fault zone. Some of the larger blocks are shown in Fig. 1.

The ultramafic rocks include serpentinized peridotite and clinopyroxenite. Meta-gabbros (Fig. 2a) are commonly associated with ultramafic blocks. The country rocks of the ultramafic blocks are migmatitic gneiss (Fig. 2b) and micaschist. All these ultramafic blocks are

flattened parallel to the regional metamorphic foliation and thus experienced likely the same deformation as their country rocks. Gabbroic cumulate, siliceous chert and chromite are not found.

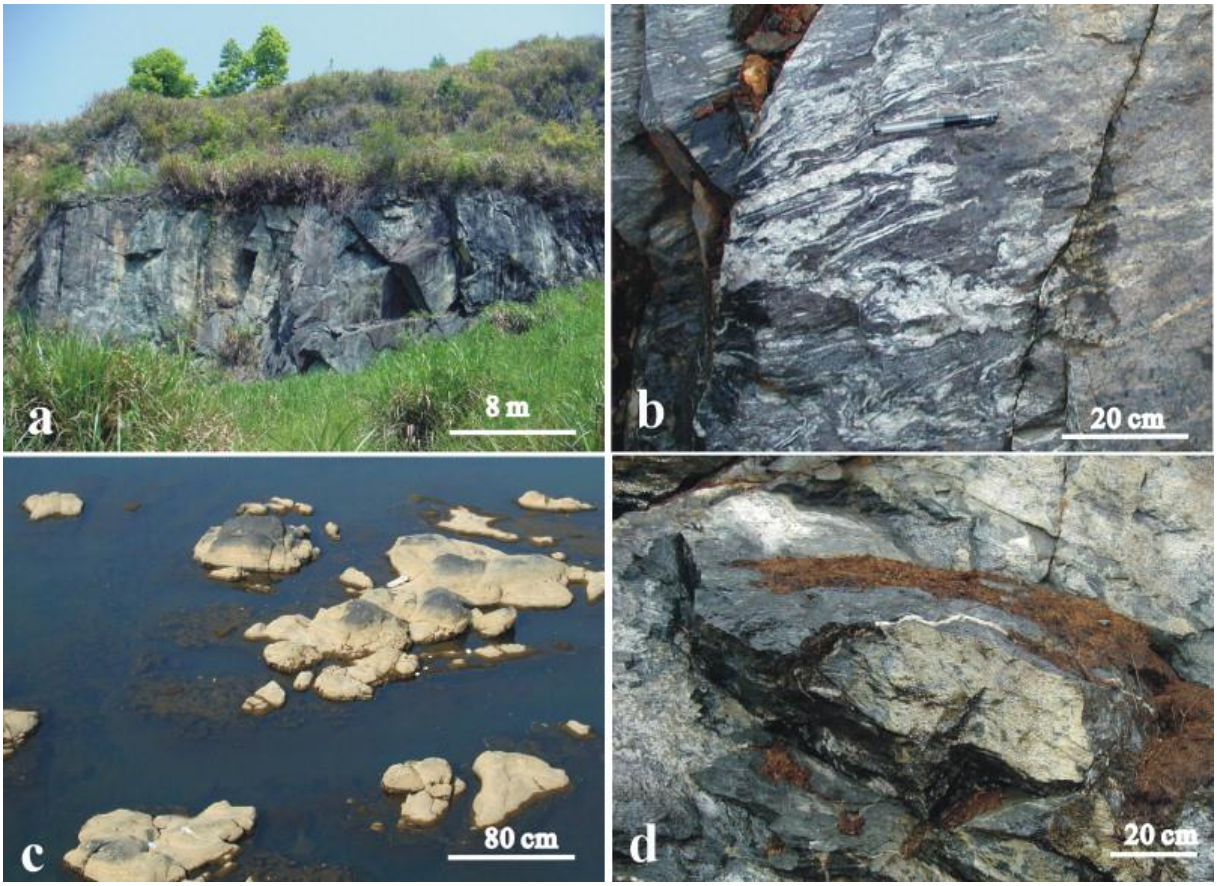

Fig. 2. Field photos of the ultramafic–mafic rocks from the Cathaysia block, a, Serpentinite quarry (site 13 in Fig. 1); b, migmatitic country gneiss (site 13 in Fig. 1); c, pillowed basalt (site 9 in Fig. 1); d, pillowed basalt (site 10 in Fig. 1).

The largest ultramafic block, about 0.8 km^2, is exposed in Shunchang as a serpentinite mine (site 13 Fig. 1). A hundred-meter-sized block of serpentinite and meta-gabbro with layered structure is shown in Fig. 2a. This block is in contact with migmatitic gneisses of the Mamianshan Group by a ductile shearing fault. Foliation, lineation and isoclinal folds of quartz and feldspar aggregates are widely developed (Fig. 2b) in the migmatitic gneisses. The foliation exhibits an orientation of 300/80 (dip direction and dip angle) and contains a stretching lineation of 215/18 (plunge direction and plunge angle). Kinematic indicators on the XZ plane exhibit a top-to-south shearing.

Petrographically, the ultramafic rocks are serpentinized. Olivine and pyroxene relict grains of ultramafic rock are rarely observed under microscope. The gabbro and diabase contain plagioclase, diopside and magnetite, but the gabbroic texture is occasionally preserved.

Both massive and pillowed basalts are found in the upper part of the basement unit (Fig. 2c). The pillowed basalt exhibits vesicular and amygdaloidal structures. At least 6 sites are presently described (Shu et al., 2008a). A NE-trending mass of pillowed basalt, ca 200 m long and 100 m wide, is exposed near the Zhenghe–Dapu fault. The pillowed bodies have different

sizes from 85 cm to 20 cm in diameter. In spite of a weak deformation, the semi-circular shape of pillow, with a flat bottom plane and a protruding top is preserved (Fig. 2d).

3. Zircon geochronology

3.1. Sampling and analytical methods

In order to understand the origin and emplacement time of the ultramafic–mafic rocks, three gabbros (sample numbers 0412, 0472 and 1092) and one basalt (0410) were collected near the Zhenghe–Dapu fault for SHRIMP U–Pb zircon dating. The petrological features of these samples are listed in Table 1.

Table 1. Petrographical features of samples from the Cathaysia block.

Sample	**412, 412-2**	**1092**	**512**	**83**	**452**	**410**
Location	Site 7 in Fig. 1	Site 13 in Fig. 1	Site 8 in Fig. 1	Site 9 in Fig. 1	Site 9 in Fig. 1	Site 6 in Fig. 1
Texture	Medium grained, gabbroic	Fine grained, gabbroic	Intergranular	Porphyritic	Fine grained, gabbroic	Porphyritic
Structure	Massive	Massive	Massive	Massive	Massive	Amygdale
Mineralogy	Olivine (3–5%), monoclinic pyroxene (30%), labrador (50%), hornblende (5%); altered minerals: chlorite + hornblende (5–10%); accessory minerals: magnetite (3%)	Olivine (1–2%), monoclinic pyroxene (25%), labrador (45%), hornblende (10%); altered minerals: chlorite + hornblende (15%); accessory minerals: spinel (1–2), magnetite (3%)	Andesine (45%, an 35–40), hornblende (40%),biotite (5–10),quartz (5%), Fe–Ti oxides (3%)	Pyroxene (25–30%), labrador (45–50%), hornblende (5–10%), chrorite (10%); accessory minerals: spinel (1%), magnetite (3–5%)	Olivine (3–5%), pyroxene (30–35%), labrador (40–45%), hornblende (10%); altered minerals: chlorite + calcite (5–10%); accessory minerals: magnetite (3–5%)	Phenocryst: olivine (2%); pyroxene (8%), labrador (15%); aphanitic groundmasses (70–75%): feldspar + pyroxene + hornblende; amygdales: quartz + prehnite (5–8%)
Name	Gabbro	Gabbro	Diorite	Diabase	Diabase	Basalt
Sample	472	473	23-2	J0413-2	J0415-2	J0416-2
Location	Site 10 in Fig. 1	Site 10 in Fig. 1	Site 13 in Fig. 1			
Texture	Middle grained, gabbroic	Fine grained	Porphyritic	Porphyritic	Porphyritic	Porphyritic
Structure	Massive	Pillow, amygdale	Rhyolitic	Rhyolitic	Rhyolitic	Rhyolitic
Mineralogy	Pyroxene (25–30%), labrador (55%), hornblende (5–10%); accessory minerals: spinel (1%), magnetite (8%)	Phenocryst: olivine (3%); pyroxene (10%), labrador (10%); aphanitic groundmasses: feldspar + pyroxene + hornblende (65–70%); altered minerals: chlorite + iddingside + calcite (10%); amygdale: quartz + prehnite (3–5%)	Phenocrysts: potash feldspar + sanidine (10%), quartz (20%),albite (3%), biotite (3–5%) groundmass: quartz + albite (50%) scaly-like sericite (10%) accessory minerals: zircon + titanite (1–3%)	Phenocrysts: potash feldspar + sanidine (15–20%), quartz (20–25%),biotite (5%); groundmass: quartz + albite + grasses (50–55%) accessory minerals: zircon + titanite + aptite (2–4%)	Phenocrysts: potash feldspar + sanidine (15%), quartz (15%),biotite (3–5%); groundmass: quartz + albite + grasses (60–65%) accessory minerals: zircon+aptite (1–2%)	Phenocrysts: potash feldspar + sanidine (15%), quartz (15%); groundmass: quartz + albite + grasses (65–70%) accessory minerals: zircon + titanite + aptite (1–3%)
Name	Gabbro	Pillow basalt	Rhyolite	Rhyolite		

Zircon concentrates were extracted using conventional heavy liquid and magnetic separation techniques at the Jiangsu Laboratory of Petrology and Mineral Research. About 20–40 grains of zircon were obtained from 10 to 15 kg rocks for each sample. The zircon grains are 30–80 μm in diameter and were mounted in epoxy resin and polished down to half section.

The cathodo-luminescence (CL) images were obtained with a Mono CL3+ (Gatan, USA) detector attached to a scanning electron microscope (Quanta 400 FEG) at the State Key Laboratory of Continental Dynamics, Northwest University, Xi'an. Most zircon grains are light purple, transparent and euhedral to sub-euhedral. CL images show oscillatory zoning (Fig. 3), indicating that most of the zircons are of magmatic origin.

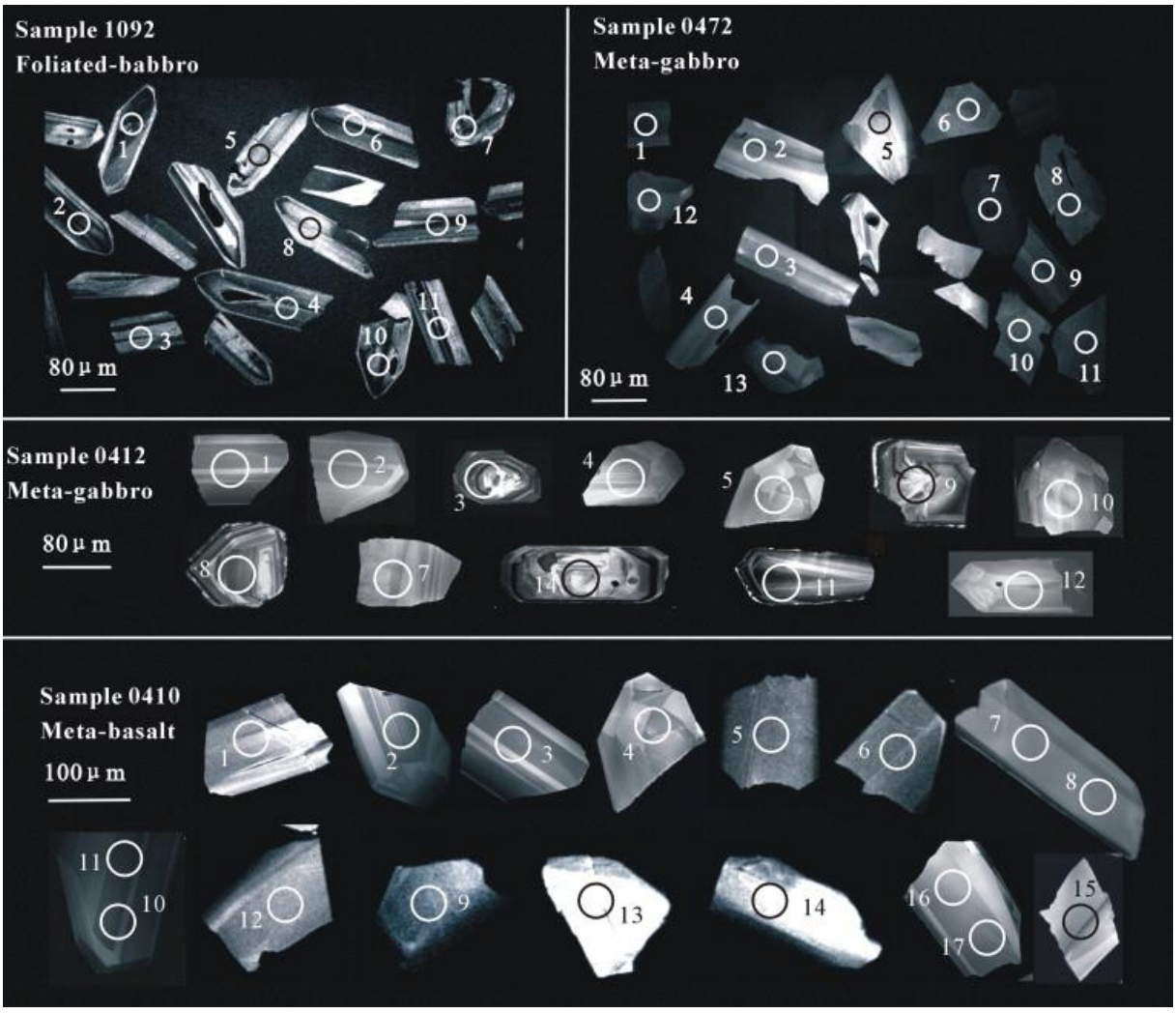

Fig. 3. CL images of zircon grains from four mafic rocks in the Cathaysia block.

All zircon U–Pb analyses were carried out in the Beijing SHRIMP Center. A 3.2 nA primary beam was used for secondary ion production. Five scans through the mass range were obtained for each spot. Ion-beam spot sizes were typically focused to ~30 μm in diameter.

The analyzing process was performed according to the procedure described by Compston et al. (1992) and Wang et al., 2008a and Wang et al., 2008b.

During SHRIMP dating, both Pb/U and Pb/Th ratios and absolute Pb, Th and U abundances of the standard zircons (TEM) with an age of 417 Ma (Black et al., 2003) and the standards zircon SL-13 ($^{206}Pb/^{238}U$ = 0.0928 corresponding 572 Ma, 238 ppm for ^{238}U, Williams et al., 1996) were used for the correction of isotopic fractionation and determination of U, Th, Pb contents. The ^{204}Pb was applied for the common lead correction and data reduction was done using Ludwig's SQUID 1.02 and ISOPLOT 2.49 programs (Ludwig, 2001a and Ludwig, 2001b). Uncertainties on individual analyses are quoted at the 1σ level, whereas those on pooled alignment analyses are quoted at the 95% confidence level. The analytic results are listed in Table 2.

For Neoproterozoic and younger rocks, $^{206}Pb/^{238}U$ ages are determined with higher precision than those based on $^{207}Pb/^{206}Pb$ ratios (Sircombe, 1999), so the average $^{206}Pb/^{238}U$ ages are adopted in this study.

3.2. Results of SHRIMP U–Pb zircon dating

The zircon grains of four mafic rock samples show high Th/U ratios (0.70–0.90) (Table 2). Samples 0410 (meta-basalt) (N29°35.20′, E120°22.60′; site 6 in Fig. 1) and sample 0412 (meta-gabbro) (N29°33.39′, E120°17.50′; site 7 in Fig. 1) were collected at the northeastern termination of the Cathaysia block. All the data points plot on, or near, the Concordia and define an average $^{206}Pb/^{238}U$ age of 857 ± 7 Ma for basalt (Fig. 4a), and 841 ± 12 Ma for gabbro (Fig. 4b). These ages are similar to those obtained for a gabbro dated at 858 ± 11 Ma from a neighboring area (Shu et al., 2006).

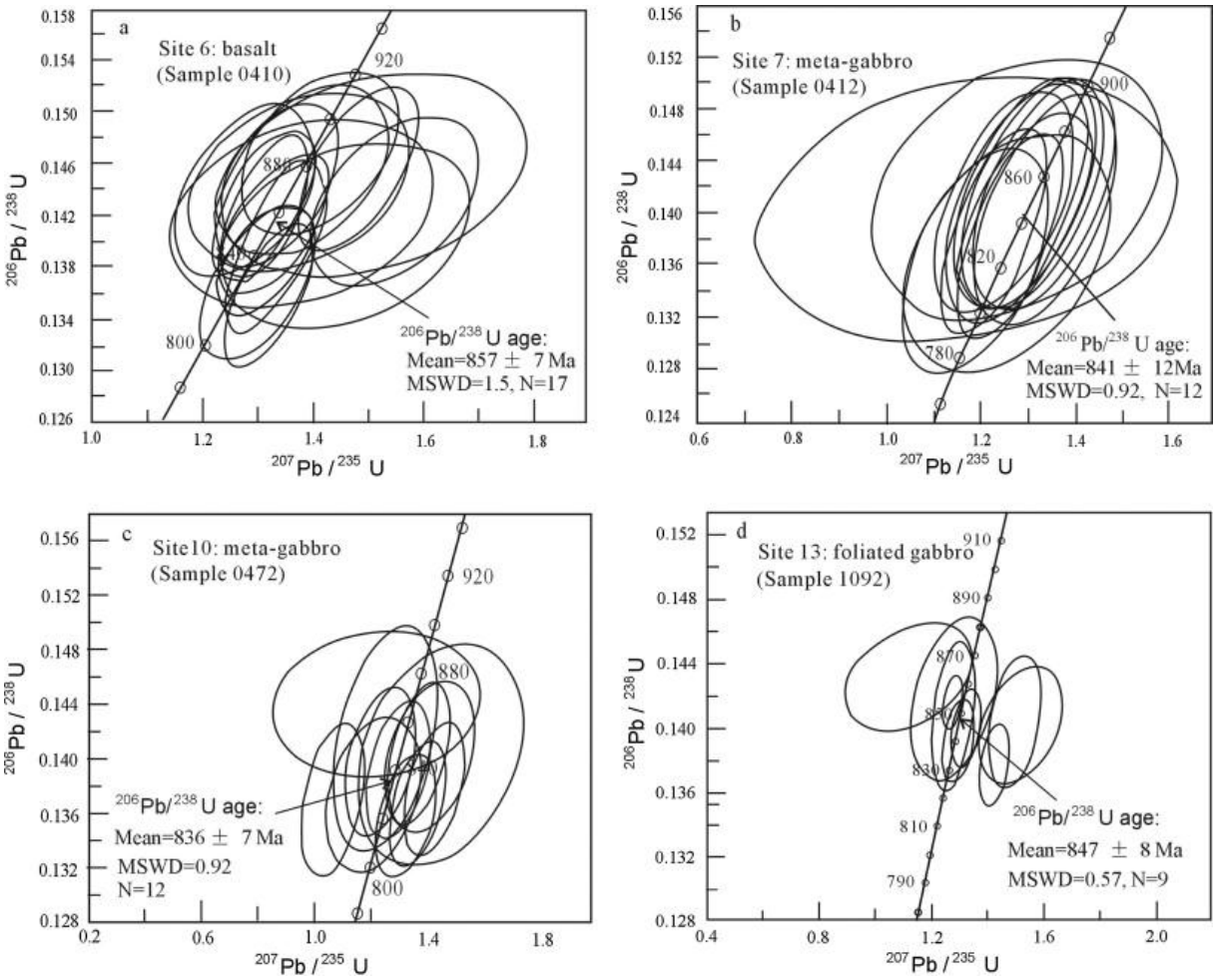

Fig. 4. U–Pb Concordia diagrams showing zircon ages of the mafic rocks.

Samples 0472 and 1092 were collected from a middle segment of the Cathaysia block close to the Zhenghe–Dapu fault zone. Sample 0472 is a massive gabbro from Zhenghe (N27°02.98′, E118°17.87′; site 10 in Fig. 1). Twelve spot analyses yielded an average ^{206}Pb/^{238}U age of 836 ± 7 Ma (Fig. 4c).

Sample 1092 is a foliated gabbro, located in site 13 in Fig. 1 (N26°54.37′, E118°03.36′). A total of 11 spot analyses were obtained, and nine analyses gave a weighted average ^{206}Pb/^{238}U age of 847 ± 8 Ma (Fig. 4d). This age is similar to that of other gabbro and basalt samples presented in this study. Moreover, sample 1092 contains a xenocrystic grain (spot 1092-7) of 1964 ± 8 Ma, suggesting the existence of an ancient basement underlying the study area. The 916 ± 5 Ma age, obtained for spot 1092-5, is presumably related to pre-Nanhua magmatism.

4. Zircon Hf isotopic study

Zircon is considered as an approximately closed system for preserving initial Lu–Hf isotopic compositions during crystallization (Woodhead et al., 2004). The Hf isotopic compositions could shed light on the nature of protolith and possible magma mixing processes (Belousova et al., 2006). To understand the petrogenesis of the mafic rocks in the Cathaysia block, six

samples were analyzed for Hf isotopic compositions. Four samples (0410, 0412, 1092, 0472) are described above, while two samples (0452 (diabase) and JW (rhyolite)), whose ages have already been published (Shu et al., 2006 and Shu et al., 2008a), are used for comparison.

4.1. Analytical procedures

In situ Lu–Hf isotope analyses were carried out on the same spots of zircon grains subjected to SHRIMP U–Pb dating. The analyses were performed using a Neptune MC-ICPMS, attached with a Geolas CQ 193 nm ArF excimer laser ablation system at the Institute of Geology and Geophysics, Chinese Academy of Sciences. This machine is a double focusing multi-collector ICPMS and has the capability of high mass resolution measurements in multiple collector modes. The analytical techniques are similar to those described in detail by Xu et al. (2004) and Wu et al. (2006).

The analyses were done with a beam size of a ca. 32 μm in diameter and a 4 Hz repetition rate. The TIMS determined value of 0.5887 for $^{176}Yb/^{172}Yb$ was applied for isobaric interference correction of ^{176}Yb on ^{176}Hf (Vervoort et al., 2004 and Wu et al., 2006). During the analytical process, the mean β_{Yb} value was used in the same spot for the interference correction of ^{176}Yb on ^{176}Hf in order to get precise data for the individual analyses. No positive linear relationship between $^{176}Yb/^{177}Hf$ and $^{176}Hf/^{177}Hf$ was observed for those high Yb/Hf samples, indicating corrections are acceptable (Wu et al., 2006). Standard zircon 91,500 with a recommended $^{176}Hf/^{177}Hf$ ratio of 0.282302 ± 8 (Goolaerts et al., 2004) was used for external correction.

Thirty-six measurements of standard 91,500 during our Lu-Hf isotope analyses in one day time yielded an average $^{176}Hf/^{177}Hf$ of 0.282293 ± 10, close to above recommended value. The $\varepsilon_{Hf}(t)$ values were calculated using a decay constant of 0.01865 Ga^{-1} for ^{176}Lu (Scherer et al., 2001) and the chondritic values ($^{176}Hf/^{177}Hf$ = 0.282772 and $^{176}Lu/^{177}Hf$ = 0.0332) of Blichert-Toft and Albarède (1997). Single-stage Hf model age (T_{DM1}) is calculated relative to the depleted mantle with present-day $^{176}Hf/^{177}Hf$ = 0.28325 and $^{176}Lu/^{177}Hf$ = 0.0384 (Nowell et al., 1998, Vervoort and Blichert-Toft, 1999 and Griffin et al., 2004). A two-stage Hf model age (T_{DM2}) is calculated based on assuming $^{176}Lu/^{177}Hf$ of average crust is 0.015 (Griffin et al., 2004 and Yu et al., 2008); for zircons with negative $\varepsilon_{Hf}(t)$ value, the model age T_{DM2} is more reasonable than the model age T_{DM1}.

4.2. Analytical results

The Lu–Hf isotopic data for 6 samples are listed in Table 3. The results suggest that zircons from four mafic samples (0410, 0412, 0472 and 1092) show very similar $(^{176}Hf/^{177}Hf)_i$ values and positive $\varepsilon_{Hf}(t)$ values, reflecting their principal derivation from a mantle-derived magma with a late Mesoproterozoic model age.

In detail, the average $(^{176}Hf/^{177}Hf)_i$ values are concentrated in a small range, in turn, 0.282354 (No. 0410), 0.282542 (No. 0412), 0.282513 (No. 0472) and 0.282525 (No. 1092). All the four analyses show positive $\varepsilon_{Hf}(t)$ values, with average of +4.1 (No. 0410), +10.5 (No. 0412), +9.3 (No. 0472), and +9.9 (No. 1092). Their average single-stage model ages (T_{DM1}, error 2σ) are 1245 ± 21 Ma, 982 ± 28 Ma, 1022 ± 21 Ma and 1006 ± 22 Ma, respectively. These features show that these zircons were crystallized from the same host magma produced from a long-term depleted mantle source.

As a comparison with the aforementioned samples, eight zircon grains from the rhyolite dated at 972 ± 8 Ma (SHRIMP U–Pb age, Shu et al., 2008b) (Sample JW, site 11 in Fig. 1) exhibit a positive $\varepsilon_{Hf}(t)$ values of +2.6 to +9.5, and their model ages (T_{DM1}) vary from 1133 Ma to 1804 Ma (Table 3). In addition, a younger diabase sample 0452 was dated at 795 ± 7 Ma (SHRIMP U–Pb age, Shu et al., 2008a). This sample contains a xenocrystic zircon grain (spot 0452-11, 992 Ma) that shows a Hf isotopic composition different from the other 11 zircon grains. The xenocryst has a negative $\varepsilon_{Hf}(t)$ value of −2.1 and an older model age (T_{DM2} = 2249 Ma).

In the diagram of εHf(t) values vs. single-stage Hf model age (T_{DM1}) (Fig. 5), except one xenocrystic grain (0452-11), almost all analyzed zircons from six samples of igneous rocks in the Cathaysia block plot in a narrow domain of 900–1400 Ma (T_{DM1}) and $\varepsilon_{Hf}(t)$ values of +1 to +13. In summary, the age and Hf isotopic data suggest that two episodes of igneous activity can be distinguished: one at ca. 800–850 Ma and another at 970 Ma.

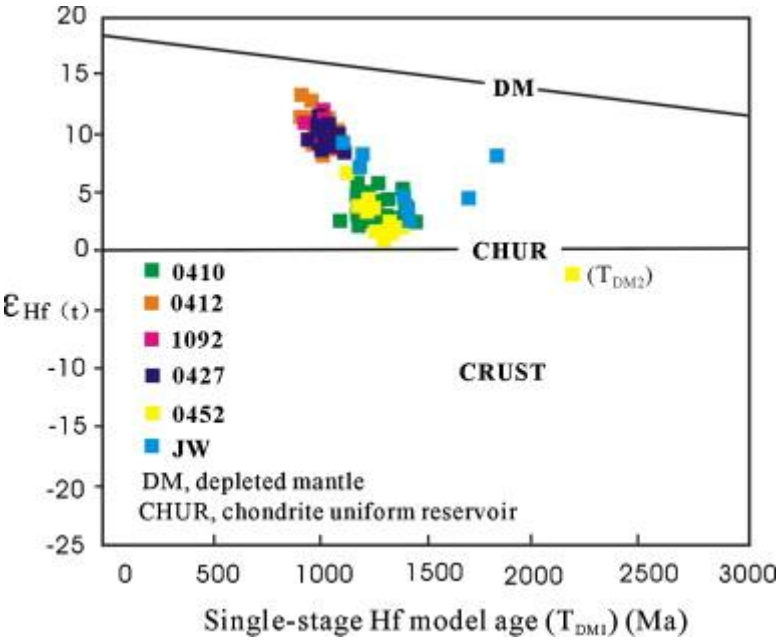

Fig. 5. Plots of **ε**Hf values vs. single-stage Hf model age (T_{DM1}) for the analyzed zircons from six samples of igneous rocks in the Cathaysia block.

5. Geochemical constraints on the Cathaysia magmatic rocks

5.1. Descriptions of the geological sections for sampling

5.1.1. Geological sections in the Zhenghe area

Near the Zhenghe–Dapu fault zone (Fig. 6a), two geological sections were constructed. The Hudiejie–Mamianshan section (Fig. 6b) shows two mafic–ultramafic blocks involved in the folding and southward thrusting of the Neoproterozoic Wudun Formation. Those blocks are bounded by ductile faults dipping 60° toward the northwest. The Hudiejie–Mamianshan section shows an asymmetric anticline composed of various blocks of serpentinite, meta-gabbro, pyroxenite, amphibole-schist, meta-basalt and marble intercalated within muscovite-

schist. Ductile planar and linear fabrics are pervasive in the schist. Muscovite grains from muscovite-schist layers occurring in the marble yield a $^{40}Ar/^{39}Ar$ plateau age of 391 ± 3 Ma (Shu, 2006), indicating the presence of an early Paleozoic tectonothermal event.

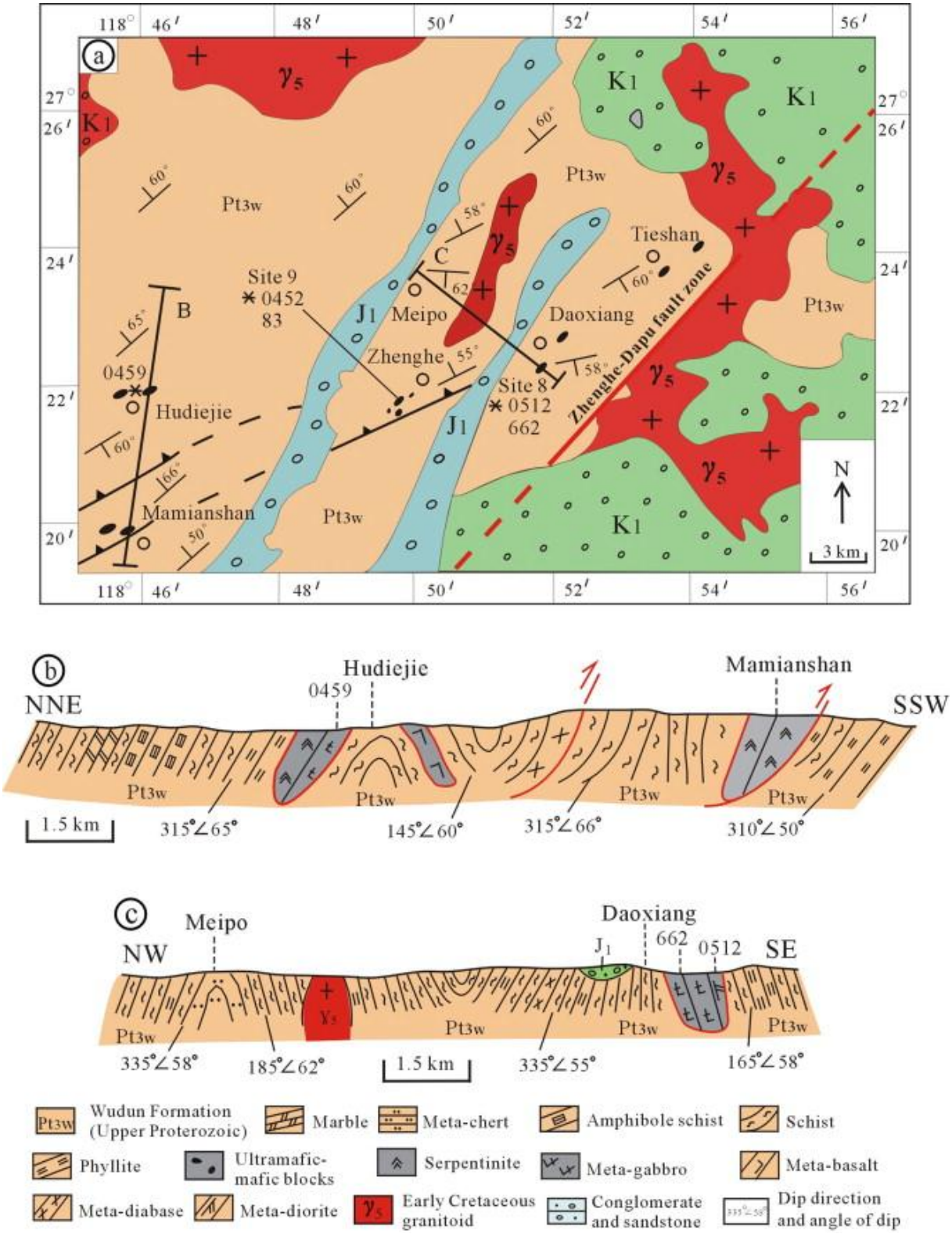

Fig. 6. Simplified geological map and two cross-sections of the Zhengh area.

The Meipo–Daoxiang section (Fig. 6c), is composed of meta-sandstone and meta-pelite of the Wudun Formation, in which a meta-gabbro block is enclosed. Most rocks have been ductilely deformed with an earlier foliation refolded by N60°E trending upright or slightly SE-verging anticlines and synclines.

5.1.2. Geological section of the Jingnan area

The Jingnan cross-section (N24°10′15″, E115°52′06″) is situated in the western segment of the study area (site 11 of Fig. 1). This section, ca 100 m thick across strike, consists of Neoproterozoic red-colored meta-rhyolite and green-colored siliceous greywacke including rhyolitic clasts. The rhyolite and greywacke are interbedded and each package is typically 3–8 m thick (Fig. 7). The rhyolite was dated at 972 ± 8 Ma by SHRIMP U–Pb zircon method (Shu et al., 2008b). Both rhyolite and greywacke show a steeply dipping foliation (320°/60–70°) and a downdip stretching lineation (325°/60–70°). The petrographic features of rhyolitic rocks are listed in Table 1.

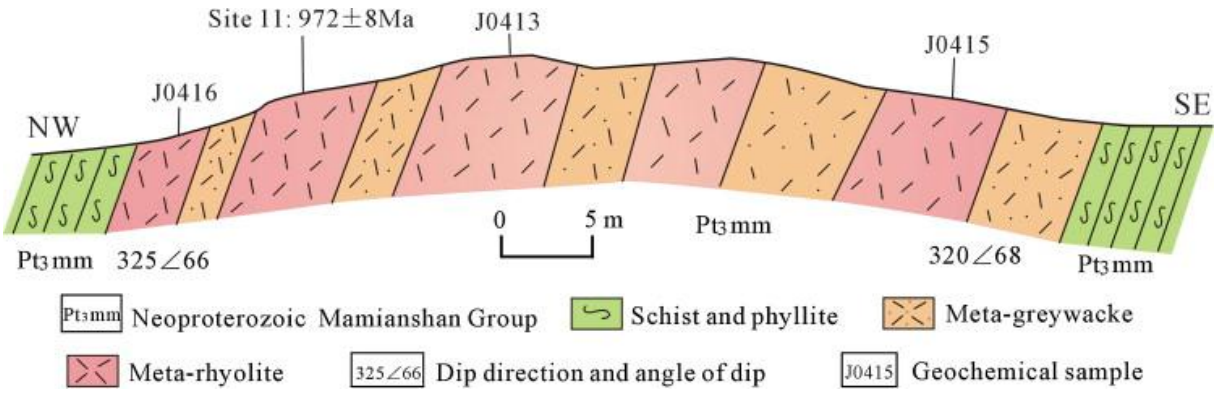

Fig. 7. Geological cross-section of the Jingnan area in the western segment of the Zhenghe–Dapu fault zone.

5.2. Samples selection and preparation

Five mafic samples (2 gabbros, 2 diabases and 1 basalt), one dioritic sample and four rhyolitic samples from the Cathaysia block were analyzed for major, REE and trace elements. The relevant petrographical features are listed in Table 1, and the sampling localities are shown in Fig. 1.

The major element compositions were analyzed using the VF-320 X-ray fluorescence spectrometer (XRF) at the Center of Modern Analysis, Nanjing University. The analytical uncertainties are estimated to be better than 5% for all the major elements; the analytical procedure is similar with that described by Franzini et al. (1972). FeO contents are analyzed by wet-chemistry method. The concentrations of rare earth and other trace elements were determined using a Finnigan MAT Element II-type ICPMS at the State Key Laboratory for Mineral Deposits Research, Nanjing University. The working conditions and analytical procedures are the same as those described by Qi and Gregoire, 2000a and Qi and Gregoire, 2000b. The analytical precision for most elements is better than 5%. The chondrite values (Sun and McDonough, 1989) are used as the representation of the REE patterns, whereas the

primitive mantle values (McDonough and Sun, 1995) are used to construct the multi-element spidergrams.

5.3. Geochemical characteristics

The analyzed results are listed in Table 4. The samples may be divided into mafic and acidic types. Five mafic samples, 0412–2, 0452, 83, 0472 and 0473, which were dated at 860–800 Ma, are high-Ti and high-K mafic rocks with TiO_2 and K_2O contents (wt% oxide) are about 2 wt% and more than 1 wt%, respectively. The four rhyolitic samples 23-2, J0413-2, J0415-2 and J0416-2, with the isotopic ages around 970 Ma, show similar major element compositions with $SiO_2 \approx 74$ wt%, $K_2O \approx 5$ wt%, $Al_2O_3 \approx 12–13$ wt% and A/CNK values around 1.10 (Table 4).

All mafic rocks show similar REE patterns with relative LREE-enrichment (Fig. 8a). Five high-Ti rocks show weak to negligible Eu anomalies (Eu/Eu* = 0.8–1.0) and have $(La/Yb)_n = 11–13$. Like the REE patterns of the Mesozoic volcanic rocks of the SE China region (Wang and Zhou, 2002), the four rhyolitic samples show remarkable negative Eu anomalies (Eu/Eu* = 0.6–0.8) (Fig. 8b) and are distinguished from typical granitic rocks with the high HREE abundances ($(Yb)_n \approx 25$).

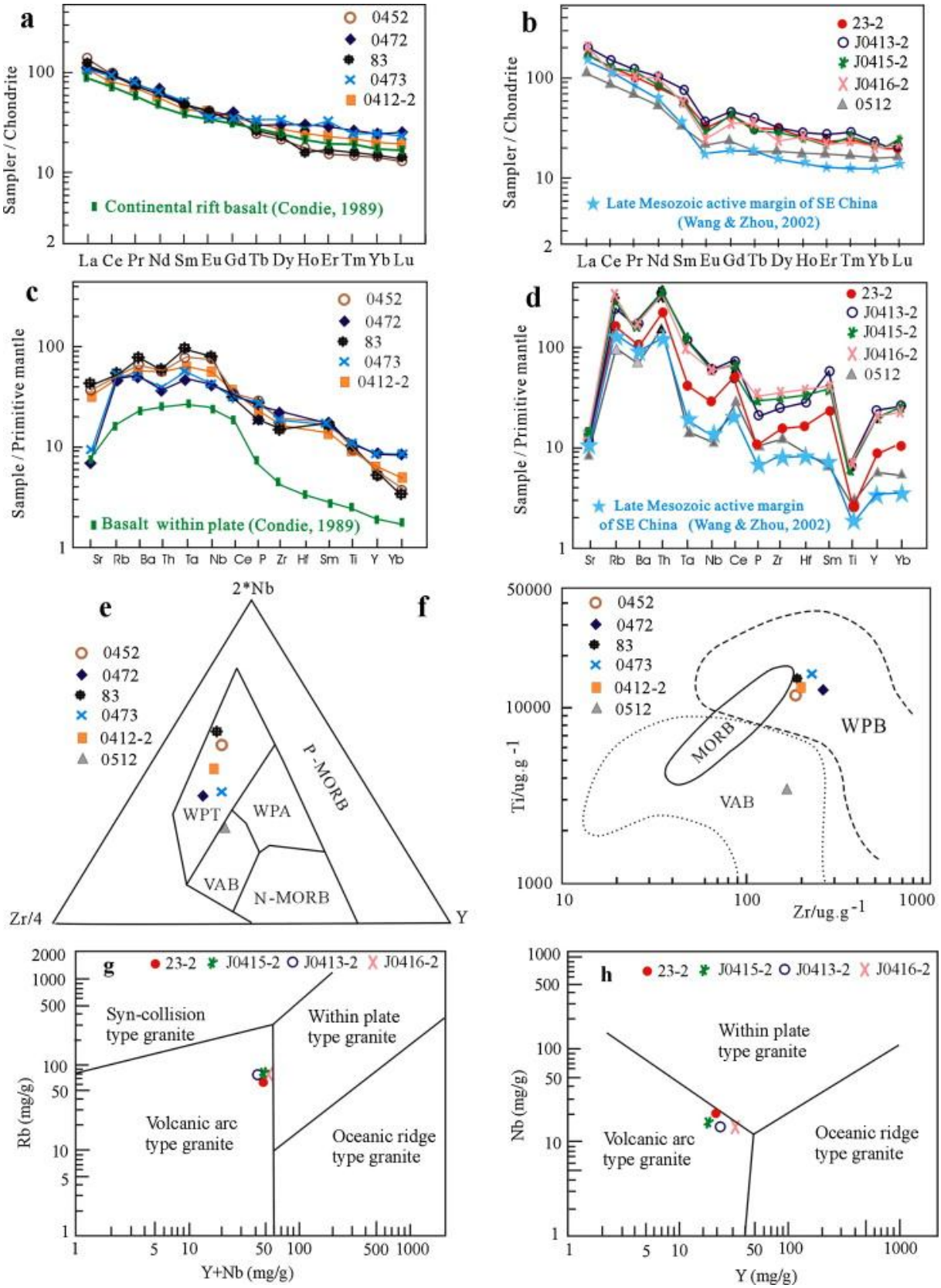

Fig. 8. Distribution of (a,b) rare earth elements, (c, d) trace elements and (e–h) tectonic setting discrimination diagrams for the mafic rocks and rhyolites from the Cathaysia block. N-MORB: normal mid-ocean ridge basalt; E-MORB: enriched mid-ocean ridge basalt; MORB: mid-ocean ridge basalt; WPT: within-plate tholeiite; WPB: within-plate basalt; VAB: volcanic arc basalt.

The high-Ti mafic rocks show distinct spidergrams (Fig. 8c) and are characterized by low abundances of Rb, Th, and enrichment in Nb, Ta and Ti. Thus, the high-Ti rocks have geochemical characteristics of continental rift or "within-plate" basalts (Condie, 1989).

The spidergrams of the rhyolitic samples (Fig. 8d) exhibit enrichment in Rb and Th, depletion in Sr, Ti and Nb–Ta. Overall, the distribution patterns are similar to that of the Late Mesozoic volcanic zone of the SE China Coastal Region, but the abundances are distinctly higher.

Consequently, the mafic and rhyolitic rocks were probably formed in two distinct tectonic settings. This is further corroborated in the discrimination diagrams of tectonic setting established from geochemical analyses. In the discrimination diagrams of Pearce et al. (1995), five high-Ti samples plot in the field of within-plate tholeiite (WPT) (Fig. 8e) or within-plate basalt (WPB) (Fig. 8f), while the dioritic sample (0512), likely the four rhyolitic samples above, falls in the field of volcanic-arc basalt (VAB) in both diagrams.

In the Rb vs (Y+Nb) and the Nb vs.Y tectonic setting discrimination diagrams, the rhyolite samples plot in the volcanic arc type granite field (Fig. 8g and h). Combining these new data with other results (Li et al., 2010b), a volcanic arc type magmatism likely took place in the Cathaysia block during the early Neoproterozoic time.

6. Discussion

6.1. Timing and episodes of magmatism in the Cathaysia basement

Combining the present results with the published isotopic ages for the igneous rocks that occur in the Cathaysia block, i.e. 858 ± 11 Ma for the meta-gabbro (SHRIMP U–Pb zircon, Shu et al., 2006), 818 ± 9 Ma for the meta-rhyolite (SHRIMP U–Pb zircon, Li et al., 2005), 800 ± 14 Ma for the felsic volcanic rocks (SHRIMP U–Pb zircon, Li et al., 2010b), 795 ± 7 Ma for the diabase (SHRIMP U–Pb zircon, Shu et al., 2008a), 839 ± 7 Ma for the diorite (SHRIMP U–Pb zircon, Li et al., 2010b), and 972 ± 8 Ma for the meta-rhyolite (SHRIMP U–Pb zircon, Shu et al., 2008b), we may conclude that (1) two important tectono-magmatic episodes occurred in the Cathaysia block during the Neoproterozoic, at ca. 970 Ma and ca. 850–800 Ma; (2) except one xenocrystic zircon grain (0452-11) dated at 992 Ma (Shu et al., 2008a), the zircons from mafic rocks in the Cathaysia block are characterized by positive $\varepsilon_{Hf}(t)$ values, suggesting a petrogenesis from the same host magma produced from a long-term depleted mantle source.

6.2. Contrasted tectonic settings for the two types of igneous rocks

Several lines of evidence, such as: (1) absence of gabbroic cumulates and chromite-bearing ultramafic rocks, (2) absence of deep-marine sedimentary rocks such as siliceous chert and turbidite, (3) distinct time difference between the mafic–ultramafic blocks (860–800 Ma, this study) and the country-rock (schist and gneiss with 1.8–1.9 Ga protolith age, Yu et al., 2009), suggest that the mafic–ultramafic rocks are not members of an ophiolitic suite.

Two types of igneous rocks have been recognized: mafic–ultramafic rocks, formed during the 860–800 Ma interval, are related to a rift setting, whereas the rhyolitic rocks were emplaced at ca. 970 Ma in a volcanic arc setting.

These geochronological and geochemical data suggest that an active continental margin developed around 970 Ma, while the 860–800 Ma period corresponds to an intra-continental rifting. The age of this Neoproterozoic rifting is consistent with the breakup of the Rodinia supercontinent (e.g. Li et al., 2008a and Li et al., 2008b, and enclosed references). Consequently, the intra-continental rifting observed in the Cathaysia block might be a response to the breakup of Rodinia. The activity of the Zhenghe–Dapu fault zone, along which mafic–ultramafic rocks dated at 860–800 Ma are widespread, likely started during the rifting stage.

6.3. A geodynamic evolution

6.3.1. Early Neoproterozoic assembly of the Yangtze block (ca 900 Ma)

The available information suggests that the time of the collision between the Yangtze and Cathaysia blocks evolved from the western, to the southeastern, and then to the eastern parts of the Yangtze block. In the western Yangtze block, Greentree et al. (2006) proposed that the sedimentary succession consisting of a coarse clastic sequence deposited in a foreland basin dated at 1000–960 Ma, corresponds to the end of the collision of the Yangtze and Cathaysia blocks.

In the southeastern Yangtze block, the timing of initial collision is a little younger than in the western Yangtze block (Shu et al., 1994, Shu and Charvet, 1996, Charvet et al., 1996, Chen et al., 1997, Zhao and Cawood, 1999, Zhou et al., 2002 and Li et al., 2009). An arc-type volcanic series, dismembered ophiolites and HP/LT blueschist mélange (site 4 of Fig. 1) are distributed along the Dongxiang–Dexing–Shexian fault zone. Three Neoproterozoic ages (sites 1–3 of Fig. 1) have been determined for the emplacement of the ophiolite: (1) 968 ± 23 Ma for an ophiolitic plagiogranite (SHRIMP U–Pb zircon; Li et al., 1994), (2) 930 ± 34 Ma for an ophiolitic gabbro (Sm–Nd isochron, Xu and Qiao, 1989), and (3) 935 ± 10 Ma for a gabbro (Sm–Nd isochron, Chen et al., 1991). These ages are also comparable with the 970 Ma age of the rhyolitic rocks from the southeastern Cathaysia block (Shu et al., 2008b).

Amphibole-bearing granites in the NE-Zhejiang Province were dated at 913 ± 15 Ma and 905 ± 14 Ma by SHRIMP zircon U–Pb (Ye et al., 2007); these ages are regarded as the time of the arc magmatism. Recently, the Xiwan leucogranite that crops out within the NE Jiangxi ophiolite yielded a zircon SHRIMP U–Pb age of 880 ± 19 Ma (Li et al., 2008a), which is interpreted as the termination of the collision between the Yangtze and Cathaysia blocks. This date is consistent with the termination of the arc magmatism at 891 ± 12 Ma (SHRIMP zircon U–Pb age from the Zhangcun rhyolite; Li et al., 2009). The collision between the Cathaysia and Yangtze blocks led to the formation of the SCB. This event should also correspond to the assembly of Rodinia (Li et al., 2002b).

6.3.2. Late Neoproterozoic continental breakup (ca 850 Ma)

Since the late Neoproterozoic, the SCB experienced a rifting event characterized by the opening of sedimentary basins and emplacement of a mafic dyke swarms (Li et al., 1999, Li et al., 2008a, Li et al., 2008b and Zheng et al., 2008). The onset of the breakup was first defined at ca. 825 Ma in the southeastern Yangtze block (Li et al., 2002a and Li et al., 2002b). However, a SHRIMP U–Pb zircon age of 849 ± 7 Ma for a dolerite dyke from northern Zhejiang (Li et al., 2009) and another zircon age of 849 ± 6 Ma for a felsic volcanic rock of

the Zhenzhushan Formation from northeastern Jiangxi (Li et al., 2010a) were recently considered by these authors as the earliest anorogenic magmatism in the Yangtze block. The geochronological results provided in this paper, ranging around 850 Ma, are consistent with the second view, suggesting that the post-collision tectono-magmatism or the earliest anorogenic magmatism in the SCB likely started from ca. 850 Ma.

This late Neoproterozoic extensional event had been documented by geochemical and geochronological data. The contemporaneous volcanic rocks and S-type granites exposed in the suture zone between the Yangtze and Cathaysia blocks argue for the timing. In the eastern segment of the SCB, a felsic volcanic rock has been dated at 797 ± 11 Ma (zircon U–Pb; Li et al., 2003b); the basalt and rhyolite were dated at 794 ± 9 Ma and 792 ± 5 Ma, respectively (zircon U–Pb; Li et al., 2009); and the peraluminous granite intruding the Neoproterozoic ophiolitic mélange yielded a zircon U–Pb age of 825 ± 3 Ma (site 5 in Fig. 1). In the middle segment of the SE Yangtze block, near Pingxiang (Fig. 1), an S-type granite was dated at 828 ± 8 Ma (zircon U–Pb; Shu et al., 2008a). Furthermore, the NW striking diabase dykes in the Pingxiang area yielded a zircon U–Pb age of 812 ± 5 Ma (Wang et al., 2006). In the western part of the SE Yangtze block, various S-type granitic plutons yield Neoproterozoic ages (LA ICPMS zircon U–Pb), for example, 819 ± 9 Ma (Li XH, 1999), 823 ± 4 Ma and 794 ± 8 Ma (Wang et al., 2006).

Thus, the 850–790 Ma interval represents the post-collisional period in the Yangtze block. This timing is consistent with the 860–795 Ma ages obtained from the mafic rocks in the Cathaysia block shown in this study. In other words, a tectono-magmatic process had taken place in the whole SCB during the late Neoproterozoic, around 860 and 790 Ma.

Moreover, during the Neoproterozoic Nanhua Period, several rift-related intra-continental sedimentary basins, coeval with a bimodal magmatism, formed in many places of South China. For example, the NE–SW trending Nanhua basin and the N-S trending Kangdian basin were opened between 820 Ma and 690 Ma (Wang and Li, 2003 and Li et al., 2002a). The description of the evolution of these basins is beyond the scope of this paper. However, we suggest that the mafic–ultramafic rocks exposed along the NE–SW trending Zhenghe–Dapu fault zone might also be a part of the Neoproterozoic Nanhua rift, which would have been ca. 600 km long and 20–30 km wide.

This Zhenghe–Dapu rift basin was filled with a chaotic sedimentation with dismembered or lens-shaped beds. The ultramafic blocks, pillow basalts, gabbros and dykes, acidic volcanic rocks, or more generally, the bimodal igneous rocks such as those exposed in the Zhenghe area, were emplaced and partly accumulated in this basin. The age of initial sedimentation within the Zhenghe–Dapu rift basin can roughly be estimated around 860 Ma. Furthermore, all the rocks deposited in this rift basin were ductilely deformed and metamorphosed during the early Paleozoic intra-continental orogeny of South China (Faure et al., 2009 and Li et al., 2010b)

The evolution of the Neoproterozoic basins in South China is similar to that of the Adelaide rift system in southeastern Australia (Li et al., 1995, Li et al., 1996 and Wang and Li, 2003), the SCB was presumably situated adjacent to eastern Australia in the Rodinian supercontinent, and it was later rifted from Australia in the Neoproterozoic (Li et al., 2008b). It is concluded that the Cathaysia, Yangtze, and southeastern Australian blocks show much similarity in terms of the Neoproterozoic magmatism and stratigraphic successions. They were certainly important components of the Rodinia supercontinent.

Acknowledgements

The reviewer Dr. Z.X. Li and the anonymous reviewer are thanked for their constructive comments and suggestions that led to a major improvement of the manuscript. We are grateful to Profs. D. Chew and X.L. Wang for their critical and constructive review and help in improving the English text. We wish to express our gratitude to Profs. B. Song and W.S. Wan for SHRIMP zircon U–Pb analyses, and Dr. Y.H. Yang for his guidance during the zircon Hf isotopic study. This research was supported by National Natural Science Foundation of China (Nos. 40634022, 40972132), the State Key Laboratory for Mineral Deposits Research of Nanjing University (No. 2008-I-01) and the State Key Laboratory of Continental Dynamics of Northwest University.

References

L.P. Black, S.L. Kamo, I.S. Williams, R. Mundil, D.W. Davis, R.J. Korsch, C. Foudoulis
The application of SHRIMP to Phanerozoic geochronology: a critical appraisal of four zircon standards
Chem. Geol., 200 (2003), pp. 171–188

E.A. Belousova, W.L. Griffin, S.Y. O'Reilly
Zircon crystal morphology, trace element signatures and Hf isotope composition as a tool for petrogenetic modeling. Examples from eastern Australian granitoids
J. Petrol., 47 (2006), pp. 329–353

J. Blichert-Toft, F. Albarède
The Lu–Hf geochemistry of chondrites and the evolution of the mantle–crust system
Earth Planet. Sci. Lett., 148 (1997), pp. 243–258

J. Charvet, L.S. Shu, Y.S. Shi, L.Z. Guo, M. Faure
The building of South China: collision of Yangzi and Cathaysia blocks, problems and tentative answers
J. Southeast Asian Earth Sci., 13 (1996), pp. 223–235

J. Charvet, L.S. Shu, M. Faure, F. Choulet, B. Wang, H.F. Lu, N. Le Breton
Structural development of the Lower Paleozoic belt of South China: genesis of an intracontinental orogen
J. Asian Earth Sci., 39 (2010), pp. 309–330

J.F. Chen, K.A. Foland, F.M. Xing, T.X. Zhou
Magmatism along the southeast margin of the Yangzi block: Precambrian collision of the Yangzi and Cathaysia blocks of China
Geology, 19 (1991), pp. 815–818

X. Chen, D.B. Rowley, J.Y. Rong, J. Zhang, Y.D. Zhang, R.B. Zhan
Late Precambrian through Early Paleozoic stratigraphic and tectonic evolution of the Nanling region, Hunan Province, South China
Int. Geol. Rev., 39 (1997), pp. 469–478

X. Chen, Y.D. Zhang, J.X. Fan, J.F. Cheng, Q.J. Li
Ordovician graptolite-bearing strata in southern Jiangxi with a special reference to the Kwangsian Orogeny
Sci. China (Earth Sci.), 53 (2010), pp. 1602–1610

W. Compston, I.S. Williams, J.L. Kirchvink
Zircon U–Pb ages for the Early Cambrian time scale
J. Geol. Sci., Lond., 149 (1992), pp. 171–184

K.C. Condie
Plate tectonics and Crustal Evolution
Pergamon Press, Oxford (1989) 476p

M. Faure, L.S. Shu, B. Wang, J. Charvet, F. Choulet, P. Monié
Intracontinental subduction: a possible mechanism for the Early Palaeozoic Orogen of SE China
Terre Nova, 21 (2009), pp. 360–368

FBGMR: Fujian Bureau of Geology and Mineral Resources, 1985. Regional Geology of Fujian Province. Geological Publishing House, Beijing, p. 617 (in Chinese with English abstract).

M. Franzini, L. Leoni, M. Saitta
A simple method to valuate the matrix effect in X-ray fluorescence analysis
X-ray Spectrom., 1 (1972), pp. 151–154

X. Gan, H. Li, D. Sun, W. Jin, F. Zhao
A geochronological study on early Proterozoic granitic rocks, southeastern Zhejiang
Acta Petrol. Mineral., 14 (1) (1995), pp. 1–8 (in Chinese with English abstract)

A. Goolaerts, N. Mattielli, J. de Jong, D. Weis, J.S. Scoates
Hf and Lu isotopic reference values for the zircon standard 91500 by MC-ICP-MS
Chem. Geol., 206 (2004), pp. 1–9

F.M. Gradstein, J.G. Ogg, A.G. Smith, W. Bleeker, L.J. Lourens
A new geologic time scale with special reference to Precambrian and Neogene
Episodes, 27 (2004), pp. 83–100

M.R. Greentree, Z.X. Li, X.H. Li, H. Wu
Late Mesoproterozoic to earliest Neoproterozoic basin record of the Sibao orogenesis in western South China and relationship to the assembly of Rodinia
Precambrian Res., 151 (2006), pp. 79–110

W.L. Griffin, E.A. Belousova, S.R. Shee, N.J. Pearson, S.Y. O'Reilly
Archean crustal evolution in the northern Yilgarn Craton: U–Pb and Hf-isotope evidence from detrital zircons
Precambrian Res., 131 (2004), pp. 231–282

L.Z. Guo, Y.S. Shi, H.F. Lu, R.S. Ma, H.G. Dong, S.F. Yang
The pre-Devonian tectonic patterns and evolution of South China

J. Southeast Asian Earth Sci., 3 (1989), pp. 87–93

P.F. Hoffman
Did the breakout of Laurentia turn Gondwanaland inside out?
Science, 252 (1991), pp. 1409–1412

JBGMR: Jiangxi Bureau of Geology and Mineral Resources, 1984. Regional Geology of Jiangxi Province. Geological Publishing House, Beijing, p. 921 (in Chinese with English abstract).

W.X. Li, X.H. Li, Z.X. Li
Neoproterozoic bimodal magmatism in the Cathaysia Block of South China and its tectonic significance
Precambrian Res., 136 (2005), pp. 51–66

W.X. Li, X.H. Li, Z.X. Li, F.S. Lou
Obduction-type granites within the NE Jiangxi Ophiolite: Implications for the final amalgamation between the Yangtze and Cathaysia blocks
Gondwana Res., 13 (2008), pp. 288–301

W.X. Li, X.H. Li, Z.X. Li
Ca. 850 Ma bimodal volcanic rocks in northeastern Jiangxi Province, South China: Initial extension during the breakup of Rodinia?
Am. J. Sci., 310 (2010), pp. 951–980

X.H. Li, G.Q. Zhou, J.X. Zhao, C.M. Fanning, W. Compston
SHRIMP ion microprobe zircon U–Pb age and Sm–Nd isotopic characteristics of the NE Jiangxi ophiolite and its tectonic implications
Chin. J. Geochem., 13 (1994), pp. 317–325

X.H. Li
Timing of the Cathaysia block formation: Constraints from SHRIMP U–Pb zircon geochronology
Episodes, 20 (1997), pp. 188–192

X.H. Li, M. Sun, G.J. Wei, C.Y Liu., Lee, J. Malpas
Geochemical and Sm–Nd isotopic study of amphibolites in the Cathaysia block, southeastern China: evidence for an extremely depleted mantle in the Paleoproterozoic
Precambrian Research, 102 (2000), pp. 251–262

X.H. Li, Z.X. Li, H. Zhou, Y. Liu, P.D. Kinny
U–Pb zircon geochronology, geochemistry and Nd isotopic study of Neoproterozoic bimodal volcanic rocks in the Kangdian Rift of South China: implications for the initial rifting of Rodinia
Precambrian Research, 113 (2002), pp. 135–154

X.H. Li, Z.X. Li, W. Ge, H. Zhou, W. Li, Y. Liu, M.T.D. Wingate
Neoproterozoic granitoids in South China: crustal melting above a mantle plume at ac 825 Ma?
Precambrian Research, 122 (2003), pp. 45–83

X.H. Li, W.X. Li, Z.X. Li, C.H. Lo, J. Wang, M.F. Ye, Y.H. Yang
Amalgamation between the Yangtze and Cathaysia blocks in South China: constraints from SHRIMP U–Pb zircon ages, geochemistry and Nd–Hf isotopes of the Shuangxiwu volcanic rocks
Precambrian Research, 174 (2009), pp. 117–128

Z.X. Li, L.H. Zhang, C.M.A. Powell
South China in Rodinia: part of the missing link between Australia–East Antarctica and Laurentia?
Geology, 23 (1995), pp. 407–410

Z.X. Li, L.H. Zhang, C.M.A. Powell
Positions of the East Asian cratons in the Neoproterozoic supercontinent Rodina
Aust. J. Earth Sci., 43 (1996), pp. 593–604

Z.X. Li, X.H. Li, P.D. Kinny, J. Wang
The breakup of Rodinia: did it start with a mantle plume beneath South China?
Earth Planet. Sci. Lett., 173 (1999), pp. 171–181

Z.X. Li, X.H. Li, H. Zho, Y. Liu, P.D. Kinny
Grenvillian continental collision in South China: new SHRIMP U–Pb zircon results and implications for the configuration of Rodinia
Geology, 30 (2002), pp. 163–166

Z.X. Li, X.H. Li, P.D. Kinny, J. Wang, S. Zhang, H. Zhou
Geochronology of Neoproterozoic syn-rift magmatism in the Yangtze Craton, South China and correlations with other continents: evidence for a mantle superplume that broke up Rodinia
Precambrian Res., 122 (2003), pp. 85–109

Z.X. Li, S.V. Bogdanova, A.S. Collins, A. Davidson, B. De Waele, R.E. Ernst, I.C.W. Fitzsimons, R.A. Fuck, D.P. Gladkochub, J. Jacobs, K.E. Karlstrom, S. Lu, L.M. Natapov, V. Pease, S.A. Pisarevsky, K. Thrane, V. Vernikovsky
Assembly, configuration, and break-up history of Rodinia: a synthesis
Precambrian Res., 160 (2008), pp. 179–210

Z.X. Li, X.H. Li, J.A. Wartho, C. Clark, W.X. Li, C.L. Zhang, C.M. Bao
Magmatic and metamorphic events during the Early Paleozoic Wuyi-Yunkai Orogeny, southeastern South China: new age constraints and P–T conditions
GSA Bull., 122 (516) (2010), pp. 772–793

H.F. Lu, D. Jia, L.S. Wang, Y.S. Shi
Tectonic evolution of the Dongshan terrane, Fujian Province, China
J. South Am. Earth Sci., 7 (1994), pp. 349–365

Ludwig, K.R., 2001a. Users Manual for Isoplot/Ex (rev.2.49): A Geochronological Toolkit for Microsoft Excel, Berkeley Geochronology Center, Spec. Publ. 1a, 55.

Ludwig, K.R., 2001b. Users manual for Isoplot/Ex rev. 2.49: A Geochronological Toolkit for Microsoft Excel. Berkeley Geochronology Centre Special Publication. 1a, 56.

W.F. McDonough, S.S. Sun
The composition of the Earth
Chem. Geol., 120 (1995), pp. 223–253

G.M. Nowell, P.D. Kempton, S.R. Noble, J.G. Fitton, A.D. Saunders, J.J. Mahoney, R.N. Taylor
High precision Hf isotope measurements of MORB and OIB by thermal ionisation mass spectrometry: insights into the depleted mantle
Chem. Geol., 149 (1998), pp. 211–233

J.A. Pearce, P.E. Baker, P.K. Harvey
Geochemical evidence for subduction fluxes, mantle melting and fractional crystallization beneath the south Sandwich island arc
J. Petrol., 36 (4) (1995), pp. 1073–1109

L. Qi, D.C. Gregoire
Determination of trace elements in twenty six Chinese geochemistry reference materials by inductively coupled plasma-mass spectrometry
Geostandards Newslett., 24 (2000), pp. 51–63

L. Qi, D.C. Gregoire
Determination of trace elements in granites by inductively coupled plasma-mass spectrometry
Talanta, 51 (2000), pp. 507–513

Rong, J.Y., Chen, X., Su, Y., Ni, Y., Zhan, R., Chen, T., Fu, L., Li, R., Fan, J., 2003. Silurian Paleogeography of China. In: Landing, E., Johnson, M. (Eds.), Silurian Lands and Seas, New York State Museum Bulletin, vol. 493. pp. 243–298.

J.Y. Rong, R.B. Zhan, H.G. Xu, B. Huang, G.H. Yu
Expansion of the Cathaysian Oldland through the Ordovician–Silurian transition: emerging evidence and possible dynamics
Sci. Chin. (D), 53 (2010), pp. 1–17

E. Scherer, C. Munker, K. Mezger
Calibration of the lutetium–hafnium clock
Science, 293 (2001), pp. 683–687

L.S. Shu, G.Q. Zhou, Y.S. Shi, J. Yin
Study of the high-pressure metamorphic blueschist and its Late Proterozoic age in the Eastern Jiangnan belt
Chin. Sci. Bull., 39 (1994), pp. 1200–1204

L.S. Shu, J. Charvet
Kinematics and geochronology of the Proterozoic Dongxiang–Shexian ductile shear zone: with HP metamorphism and ophiolitic mélange (Jiangnan Region, South China)
Tectonophysics, 267 (1996), pp. 291–302

L.S. Shu
Pre-Devonian Tectonic Evolution of South China: from Cathaysia block to Caledonian Period Folded Orogenic Belt
Geol. J. China Univ., 12 (2006), pp. 418–431 (in Chinese with English abstract)

L.S. Shu, M. Faure, S.Y. Jiang, Q. Yang, Y.J. Wang
SHRIMP zircon U–Pb age, litho- and biostratigraphic analyses of the Huaiyu Domain in South China—evidence for a Neoproterozoic orogen, not Late Paleozoic–Early Mesozoic collision
Episodes, 29 (2006), pp. 244–252

L.S. Shu, M. Faure, B. Wang, X.M. Zhou, B. Song
Late Paleozoic–Early Mesozoic Geological Features of South China: response to the Indosinian collision event in Southeast Asia
C. R. Geosci., 340 (2008), pp. 151–165

L.S. Shu, P. Deng, J.H. Yu, Y.B. Wang, S.Y. Jiang
The age and tectonic environment of the rhyolitic rocks on the western side of Wuyi Mountain, South China
Sci. Chin. (D), 51 (8) (2008), pp. 1053–1063

L.S. Shu, J.H. Yu, D. Jia, B. Wang, W.Z. Shen, Y.Q. Zhang
Early Paleozoic orogenic belt in the eastern segment of South China
Geol. Bull. Chin., 27 (10) (2008), pp. 1081–1093

L.S. Shu, X.M. Zhou, P. Deng, B. Wang, S.Y. Jiang, J.H. Yu, X.X. Zhao
Mesozoic tectonic evolution of the southeast china block: new insights from basin analysis
J. Asian Earth Sci., 34 (2009), pp. 376–391

K.N. Sircombe
Tracing provenance through the isotope ages of littoral and sedimentary detrital zircon, eastern Australia
Sedim. Geol., 124 (1999), pp. 47–67

S.S. Sun, W.F. McDonough
Chemical and isotopic systematics of oceanic basalts: implications for mantle composition and processes
A.D Saunders, M.J. Norry (Eds.), J. Geol. Soc. London, Spec. Publ., 42 (1989), pp. 313–345

J.D. Vervoort, J. Blichert-Toft
Evolution of the depleted mantle: Hf isot588 ope evidence from juvenile rocks through time
Geochim. Cosmochim. Acta, 63 (3–4) (1999), pp. 533–556

J.D. Vervoort, P.J. Patchett, U. Soderlund, M. Baker
Isotopic composition of Yb and the determination of Lu concentrations and Lu/Hf ratios by isotopic dilution using MC-ICPMS
Geochem. Geophys. Geosyst., 5 (2004) 2004GC000721

Y. Wan, D. Liu, M. Xu, J. Zhuang, B. Song, Y. Shi, L. Du

SHRIMP U–Pb zircon geochronology and geochemistry of metavolcanic and metasedimentary rocks in NW Fujian, Cathaysia block, China: tectonic implications and the need to redefine lithostratigraphic units
Gondwana Res., 12 (1–2) (2007), pp. 166–183

D.Z. Wang, X.M. Zhou
Genesis of Late Mesozoic volcanic-intrusive Complex of Southeast China and Crustal Evolution
Science Press, Beijing (2002) (in Chinese with English abstract) 295p

H.Z. Wang, X.X. Mo
An outline of the tectonic evolution of China
Episodes, 18 (1995), pp. 6–16

L.J. Wang, J.H. Yu, S.Y. O'Reilly, W.L. Griffin, Z.Y. Wei, S.Y. Jiang, T. Sun.
Grenvillian orogeny in the Southern Cathaysia block: constraints from U–Pb ages and Lu–Hf isotopes in zircon from metamorphic basement
Chin. Sci. Bull., 53 (19) (2008), pp. 3037–3050

J. Wang, Z.X. Li
History of Neoproterozoic rift basins in South China: implications for Rodinia break-up
Precambrian Res., 122 (1–4) (2003), pp. 141–158

X.L. Wang, J.C. Zhou, J.S. Qiu, W.L. Zhang, X.M. Liu, G.L. Zhang
LA-ICP-MS U–Pb zircon geochronology of the Neoproterozoic igneous rocks from Northern Guangxi Province, South China: implications for the tectonic evolution
Precambrian Res., 145 (2006), pp. 111–130

X.L. Wang, J.C. Zhou, J.S. Qiu, S.Y. Jiang, Y.R. Shi
Geochronology and geochemistry of Neoproterozoic mafic rocks from western Hunan, South China: implications for petrogenesis and post-orogenic extension
Geol. Mag., 145 (2) (2008), pp. 215–233

Y.J. Wang, W.M. Fan, F. Guo, T.P. Peng, C.W. Li
Geochemistry of Mesozoic mafic rocks adjacent to the Chenzhou–Wulin fault, South China: implications for the lithospheric boundary between the Yangtze and the Cathaysia blocks
Int. Geol. Rev., 45 (2003), pp. 263–286

Y.J. Wang, W.M. Fan, G.C. Zhao, S.C. Ji, T.P. Peng
Zircon U–Pb geochronology of gneisses in Yunkai Mountains and its implications on the Caledonian event in South China
Gondwana Res., 12 (4) (2007), pp. 404–416

I.S. Williams, I.S. Buick, I. Cartwright
An extended episode of early Mesoproterozoic metamorphic fluid flow in the Reynolds Range, central Australia
J. Metamorphic Geol., 14 (1996), pp. 29–47

J. Woodhead, J. Hergt, M. Shelley, S. Eggins, R. Kemp

Zircon Hf-isotope analysis with an excimer laser, depth profiling, ablation of complex geometries, and concordant age estimation
Chem. Geol., 209 (2004), pp. 121–135

F.Y. Wu, Y.H. Yang, L.W. Xie, J.H. Yang, P. Xu
Hf isotopic compositions of the standard zircons and baddeleyites used in U–Pb geochronology
Chem. Geol., 234 (2006), pp. 105–126

L. Xiang, L.S. Shu
Predevonian tectonic evolution of the eastern South China block: geochronological evidence from detrital zircons
Sci. Chin. (Earth Sci.), 53 (2010), pp. 1427–1444

W.J. Xiao, H.Q. He
Early Mesozoic thrust tectonics of the northwest Zhejiang region (Southeast China)
GSA Bull., 117 (2005), pp. 1–17

B. Xu, G.S. Qiao
Sm–Nd isotopic age and tectonic setting of the Late Proterozoic ophiolites in Northeastern Jiangxi Province
J. Nanjing Univ. (Earth Sci.), 3 (1989), pp. 108–114 (in Chinese with English abstract)

P. Xu, F.Y. Wu, L.W. Xie, Y.H. Yang
Hf isotopic compositions of the standard zircons for U–Pb dating
Chin. Sci. Bull., 49 (2004), pp. 1642–1648

X.S. Xu, S.Y. O'Reilly, W.L. Griffin, P. Deng, N.J. Pearson
Relict Proterozoic basement in the Nanling mountains (SE China) and its tectonothermal overprinting
Tectonics, 24 (2005), pp. 1–16

X.S. Xu, S.Y. O'Reilly, W.L. Griffin, X.L. Wang, N.J. Pearson, Z.Y. He
The crust of Cathaysia: age, assembly and reworking of two terranes
Precambrian Res., 158 (1–2) (2007), pp. 51–78

J.L. Yao, L.L. Shu, M. Santosh
Detrital zircon U–Pb geochronology, Hf-isotopes and geochemistry—new clues for the Precambrian crustal evolution of Cathaysia block, South China
Gondwana Res. (2011) http://dx.doi.org/10.1016/j.gr.2011.01.005

M.F. Ye, X.H. Li, W.X. Li, Y. Liu, Z.X. Li
SHRIMP zircon U–Pb geochronological and whole-rock geochemical evidence for an early Neoproterozoic Sibaoan magmatic arc along the southeastern margin of the Yangtze Block
Gondwana Res., 12 (2007), pp. 144–156

H. Yu
Structural stratigraphy and basin subsidence of Tertiary basins along the Chinese southeastern continental margin

Tectonophysics, 235 (1994), pp. 63–76

J.H. Yu, X.M. Zhou, S.Y. O'Reilly, L. Zhao, W.L. Griffin, R.C. Wang
Formation history and protolith characteristics of granulite facies metamorphic rock in Central Cathaysia deduced from U–Pb and Lu–Hf isotopic studies of single zircon grains
Chin. Sci. Bull., 50 (2005), pp. 2080–2089

J.H. Yu, Y.S. O'Reilly, L.J. Wang, W.L. Griffin, S.Y. Jiang, R.C. Wang, X.S. Xu
Finding of ancient materials in Cathaysia and implication for the formation of Precambrian crust
Chin. Sci. Bull., 52 (2007), pp. 13–22

J.H. Yu, S.Y. O'Reilly, L.J. Wang, W.L. Griffin, M. Zhang, R.C. Wang, S.Y. Jiang, L.S. Shu
Where was South China in the Rodinia supercontinent? Evidence from U–Pb ages and Hf isotopes of detrital zircons
Precambrian Res., 164 (1–2) (2008), pp. 1–15

J.H. Yu, L.J. Wang, W.L. Griffin, S.Y. O'Reilly, M. Zhang, C.Z. Li, L.S. Shu
A Paleoproterozoic orogeny recorded in a long-lived cratonic remnant (Wuyishan terrane), eastern Cathaysia block, China
Precambrian Res., 174 (2009), pp. 347–363

S.G. Zhang, H.J. Yan
A brief introduction to international stratigraphic chart and global stratotype section and points
J. Stratigr., 29 (2005), pp. 188–203

G. Zhao, P. Cawood
Tectonothermal evolution of the Mayuan assemblage in the Cathaysia block: implications for neoproterozoic collision-related assembly of the South China Craton
Am. J. Sci., 299 (1999), pp. 309–339

Y.F. Zheng, R.X. Wu, Y.B. Wu, S.B. Zhang, H. Yuan, F.Y. Wu Rift melting of juvenile arc-derived crust: geochemical evidence from Neoproterozoic volcanic and granitic rocks in the Jiangnan Orogen, South China Precambrian Res., 163 (2008), pp. 351–383

J.C. Zhou, X.L. Wang, J.S. Qiu, J.F. Gao Geochemistry of Meso- to Neoproterzoic mafic–ultramafic rocks from northern Guangxi, China: arc or plume magmatism? Geochem. J., 38 (2004), pp. 139–152

J.C. Zhou, X.L. Wang, J.S. Qiu Geochronology of Neoproterozoic mafic rocks and sandstones from northeastern Guizhou, South China: Coeval arc magmatism and sedimentation Precambrian Res., 170 (2009), pp. 27–42

M.F. Zhou, D.P. Yan, A.K. Kennedy, Y. Li, J. Ding SHRIMP U–Pb zircon geochronological and geochemical evidence for Neoproterozoic arc-magmatism along the western margin of the Yangtze block, South China Earth Planet. Sci. Lett., 196 (2002), pp. 51–67

X.M. Zhou, Y.H. Zhu Late Proterozoic collisional orogen and geosuture in southeastern China: petrological evidences Chin. J. Geochem., 12 (3) (1993), pp. 239–251